International Journal of Engineering, Mathematical and Physical Sciences
ISSN: 2517-9934
Vol:10, No:3, 2016

First-Principles Density Functional Study of Nitrogen-Doped P-Type ZnO

Abdusalam Gsiea, Ramadan Al-habashi, Mohamed Atumi, Khaled Atmimi

Abstract—We present a theoretical investigation on the structural, electronic properties and vibrational mode of nitrogen impurities in ZnO. The atomic structures, formation and transition energies and vibrational modes of $(NO_3)_i$ interstitial or NO_4 substituting on an oxygen site ZnO were computed using ab initio total energy methods. Based on Local density functional theory, our calculations are in agreement with one interpretation of bound-excition photoluminescence for N-doped ZnO. First-principles calculations show that $(NO_3)_i$ defects interstitial or NO_4 substituting on an Oxygen site in ZnO are important suitable impurity for p-type doping in ZnO. However, many experimental efforts have not resulted in reproducible p-type material with N_2 and N_2O doping. by means of first-principle pseudo-potential calculation we find that the use of NO or NO_2 with O gas might help the experimental research to resolve the challenge of achieving p-type ZnO.

Keywords—Density functional theory, nitrogen, p-type, ZnO.

I. Introduction

ZINC oxide is a transparent semiconductor with a direct, wide band-gap of 3.4 eV and large exciton binding energy of 60 meV. This has lead to ZnO being proposed for applications such as optoelectronic devices, lasers and light emitting diodes [1]-[4]. The most significant impediment to the widespread exploitation of ZnO-related materials in electronic and photonic applications is the difficulty in carrier doping, specifically as it related to achieving p-type material. Perhaps the most promising and commonly dopants for p-type ZnO is the nitrogen element, although theoretical studies signified a difficulty to explain the p-type activity for nitrogen at room temperature [5], [6]. Nevertheless, high hole carrier concentrations from N impurities (10^{17}–$10^{19}\,\mathrm{cm}^{-3}$) have been achieved experimentally [7], [8]. Some experimental works report obtaining p-type ZnO films can be supplied by NO gas [9], [10] as the oxygen source and nitrogen dopand; on the other hand, nitrogen ZnO films produce n-type conduction by using an N_2 or NH_3 [9], [10]. An important characteristic of ZnO is that it exhibits n-type conductivity even without intentional doping, and a difficulty in obtaining p-type conductivity also occurs due to carrier compensation [11]. The change of the type of conductivity when increasing temperatures can be attributed to the reevaporation of oxygen gas. There is experimental evidence supported that the candidacy of nitrogen for p-type doping [7], [12]-[17]. Furthermore, the photoluminescence from N-doped ZnO, suggestive of an acceptor levels at≈200 meV above E_v [18]-[26]. However, the location of the acceptor level is a matter of some dispute with the result of the theoretical described as a shallow which attributed to N_O which has acceptor level around of $E_v+400\,meV$ above the valance-band [26], [6], [27]. IR absorption measurements on N-doped ZnO showed several peaks ranged of significantly higher than the phonon frequencies of the ZnO host.

We present the investigation for the electronic structure of various p-type defects in ZnO by comparing the formation energies through first-principles density functional pseudopotential calculations, and discuss the chemistry that tends to enhance the formation of nitrogen with oxygen rather than other.

A. Gsiea is with the Department Physics, Tripoli University, Tripoli, Libya (e-mail: abslam_68@yahoo.com).
R. Alhabashi and M. Atumi are with Azzytuna University.

II. Method

Calculations are based upon density functional theory using the AIMPRO package [28], [29]. Defects are simulated by the use of large super-cells and periodic boundary conditions. The cells are repeats of the primitive hexagonal unit cell containing four atoms (Zn_2O_2) with lattice vectors a[1000], a[0100] and c[0001]. The calculated values for a and c are 6.18 and 9.81Å, respectively. We have analysed N-centres in supercells containing 72 or 192 atoms, comprised from $(3\times3\times2)$ and $(4\times4\times3)$ primitive cells, respectively.

The Brillouin-zone is sampled using the Monkhorst-Pack [30] scheme generally with a mesh of $2\times2\times2$ k-points. Structures are optimised via a conjugate-gradients scheme until the change in energy between iterations is less than 10^{-5}Ha.

Atoms are simulated using *ab initio* pseudopotentials [31] and the total energies and forces are obtained with a local density approximation for the exchange-correlation [32]. The wave functions and charge density are expanded in terms of Gaussian orbitals and plane-waves, respectively [33]. For the Zn, O and group V, we include s, p and d functions, with a total of 28, 28 and 32 functions per atom, respectively. Plane waves up to 150 Ha are used to expand the charge density.

We calculate the formation energy of a defect X using

$$E^f(X,q) = E^{\mathrm{tot}}(X,q) - \sum_i \mu_i + q\mu_e + \zeta(X,q), \qquad (1)$$

where $E^{\mathrm{tot}}(\mathrm{X,q})$ is the total energy calculated of the system X containing the defect in charge state q, μ_i denotes the chemical potential of species (i =Zn, O and N), $E_v(X,q)$ is the Fermi energy at the valance-band top, μ_e is the electron chemical potential, which defined as zero at the valence band top. In ZnO, the chemical potentials of components μ_{O} and μ_{Zn} are related by $E(\mathrm{ZnO}) = \mu_{\mathrm{O}} + \mu_{\mathrm{Zn}}$ where $E(\mathrm{ZnO})$ is the energy per bulk of pair in ZnO. The range of possible values for μ_{O} and μ_{Zn} is related to the requirement for ZnO to be

stable relative to decomposition into its elemental constituents, so that the zinc-rich limit is taken from zinc-metal, and for oxygen-rich limit μ_O is taken from the O_2 molecule. The heat of formation for ZnO in this way is calculated to be 3.9 eV, while experimentally is 3.61 eV [34]. The chemical potential for N is taken N_2 molecule.

For the electrical characteristics of the defect centres, we calculate the transition levels, $E(q, q\prime)$, defined as the electron chemical potential where the formation energies for two charge states, q and $q\prime$, are equal. For example, the donor level is the value of μ_e for which $E^f(X, 0) = E^f(X, +1)$, and $E^f(X, 0) = E^f(X, -1)$ for the acceptor level.

We used a potential-alignment technique [35] to calculate the electrostatic potential for 192 atoms for different structure to ensure that the two terms which entering formation energy $E_{X,q}$, E_H are accuracy.

III. Result

It is a potentially important observation that in many experiments where the source species for nitrogen doping involves N–O bonds, such as NO, NO_2 and NH_4NO_3 (ammonium nitrate), the resulting ZnO films may be activated to produce p-type carriers [9], [17], [36]-[38]. The suspicion might be that N-O bonds survive incorporation into the growing films, or even that the molecules themselves form interstitial dopants.

In addition to the preceeding molecular groups, the insertion of a nitrate ion into the lattice might result in an interstitial object, $(NO_3)_i$, or react with the oxygen host to form an exotic $(NO_4)_O$ species. A superficial view of the chemistry by which such species might be formed may involve insertion directly of nitrate ions, or from the reaction of NO_2 source species with interstitial oxygen via reactions of the type:

$$(NO_2 + O_i) \longrightarrow (NO_4)_O \tag{2}$$

and

$$NO_2 + O_i \longrightarrow (NO_3)_i. \tag{3}$$

A. Structure Details

As with previous molecular groups, the structures composed from the addition of a single N atom and three additional oxygen atoms to ZnO were obtained in two ways. The first is simple insertion of the nitrate group into the lattice at a cage site. The second was the decoration of the structure obtained for $(NO_3)_O$, as described in Section III.

Relaxation of such starting configurations was found to result in two chemically distinct structures with practiacally the same total energies. One configuration may be viewed as a modified nitrogen substitution for an O site, described as $(NO_4)_O$, depicted in Fig. 1 (a). The nitrate group was found to preferentially insert itself into a Zn–O bond (similar to the structure of interstitial N_2 molecules), and this structure is shown schematically in Fig. 1 (b).

The N-O bond lengths in $(NO_4)_O$ are calculated to be in the range of 1.34–1.37 Å which are in agreement with experimental value for a N-O single bonds in nitrates [39]. $(NO3)_i$ (Fig. 1 (b)) involves a broken Zn–O bond, with the

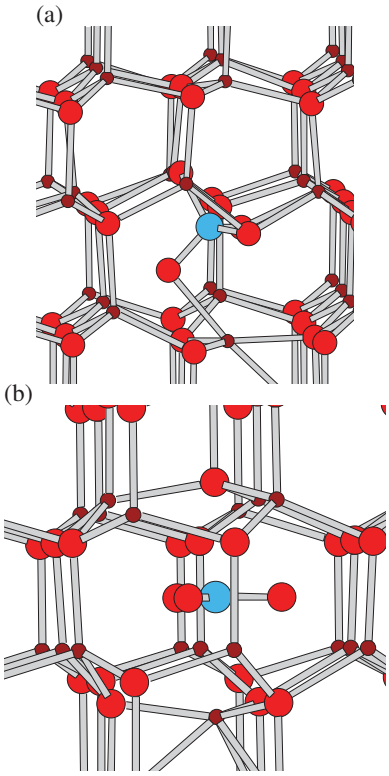

Fig. 1 Schematic structures of (a) $(NO_4)_O$ and (b) $(NO_3)_i$ in ZnO. brown, red and blue colours represent zinc, oxygen and nitrogen, respectively. The vertical and horizontal axes are [0001]

equilibrium structure having N-O bond lengths and angles calculated to be 1.25 Åand 119°, respectively, which is in good agreement with the experimental values [39] of 1.21 Å and 120° for the $(NO_3)^{1-}$ anion. The structures therefore reflect standard N-O chemistry, at least at a structural level.

The binding energy, as determined from the following reactions,

$$(NO_2)_i^{1+} + O_i^{2-} \longrightarrow (NO_4)_O^{1-} \tag{4}$$

and

$$(NO_2)_i^{1+} + O_i^{2-} \longrightarrow (NO_3)_i^{1-} \tag{5}$$

are 1.8 eV and 1.7 eV, respectively. Based upon the current data presented here, there are no reactions with smaller heats of reaction, so it seems reasonable to conclude that $(NO_4)_O^{1-}$ represents a thermodynamically stable species relative to likely dissociation products.

B. Electrical Levels

Fig. 2 shows plots of the formation energies (1) for $(NO_4)_O$ and $(NO_3)_i$. They both yield relatively shallow acceptor levels, around $E_v + 0.2$ eV for $(NO_4)_O$ and $E_v + 0.24$ eV for $(NO_3)_i$. These levels are in agreement with one interpretation of bound-exciton photoluminescence from N-doped ZnO, suggestive of an acceptor levels at ≈200 meV above E_v [21]-[26].

The acceptor level of the both structures are further illustrated in Fig. 3, which shows the band-structure along

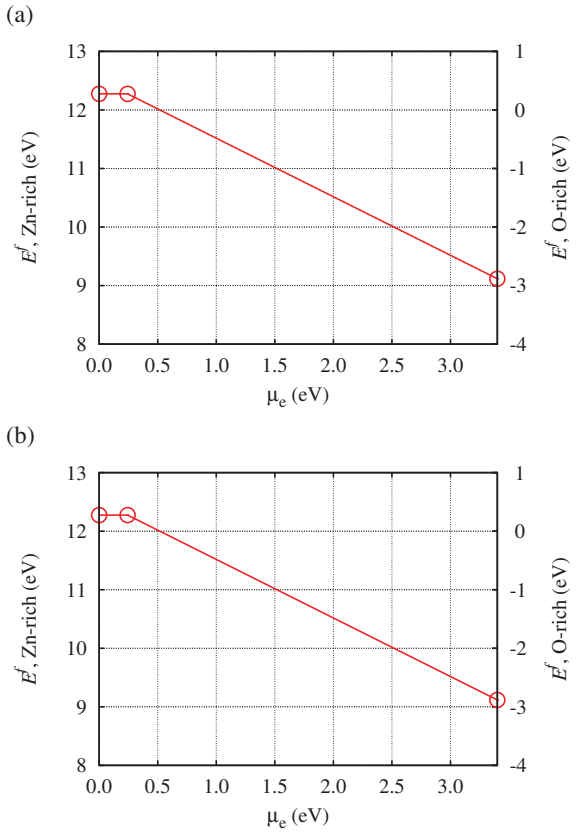

Fig. 2 E^f *vs.* μ_e for (a) $(NO_4)_O$ and (b) $(NO_3)_i$ defects in ZnO calculated using the 192 atom supercell

high symmetry directions in the Brillouin-Zone (BZ). Note the empty band is close to the valance band top, consistent with the calculated acceptor

To understand where is the empty level come from and is it the empty level is in the valance-band top, Fig. 4 illustrates the wave function distribution of Kohn-Sham orbital of the empty levels of the (NO_3) molecule and $(NO_3)_i$ defects associated to the host ZnO valance-band top, where molecule grab the electron from $2p$ orbital of the host oxygen atom.

C. Vibrational Modes

Finally, since both structures are based upon simple molecular groups, it may be fruitful to determine the vibrational frequencies that may be compared with experimental data, such as from PL.

TABLE I
THE VIBRATIONAL MODES OF $(NO_3)_i$ AND $(NO_4)_O$ cm^{-1}

Defect	f (cm^{-1})					
$(NO_3)_i$	702	1071	1384	1392	-	-
$(NO_4)_O$	703	731	929	974	989	1019

Amongst the local modes of $(NO_4)_O^{-1}$ and $(NO_3)_i^{-1}$, those calculated at 1020 cm^1 and 1392 cm^1 are in notable agreement with Raman peaks from experiment at 1150 cm^1

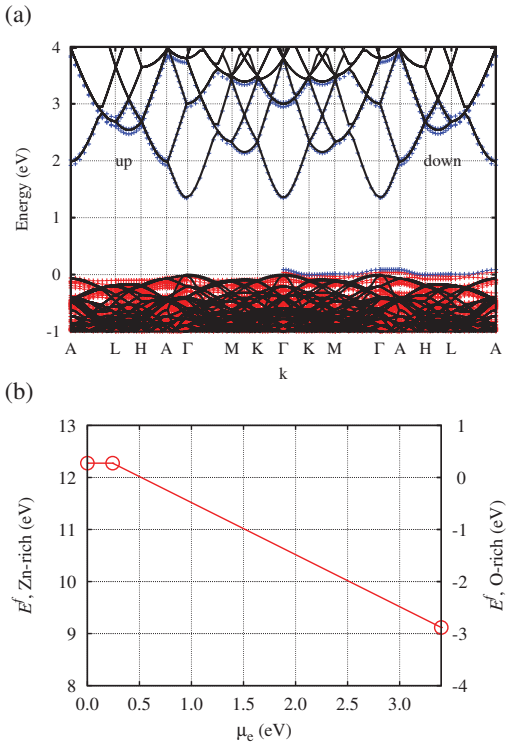

Fig. 3 Band structure of (a) $(NO_4)_O$ and (b) $(NO_3)_i$ in w-ZnO: The zero of energy is set to be the valance band top for bulk ZnO; red and blue circles indicate filled and empty bands, respectively

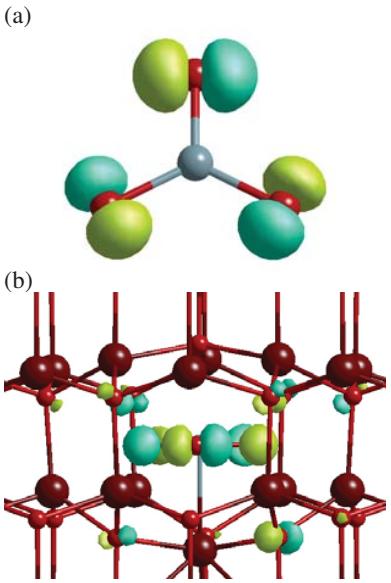

Fig. 4 Wavefunction distribution of (a) (NO_3) molecule (b) the $(NO_3)_i$ defects in ZnO calculated using the 192 atom supercell

and 1360 cm^1 [40], [41], and 1100 cm^1 and 1158 cm^1 [25]. These Raman features are not observed in the ZnO not doped with nitrogen. In particular, these peaks are observed when NO gas is used as nitrogen doped and oxygen source for nitrogen

doped ZnO [40], [41]. The local vibration modes might be related to the stretching vibration of NO molecule complex [42]. In addition, a fraction of N atoms is incorporated as NO they did not observe hydrogen related local vibrational modes such as N-H and C-H [40].

IV. Conclusion

$(NO_4)_O$ and $(NO_3)_i$ centres in ZnO present a rather appealing possible explanation for the production of p-type ZnO using N-O based doping precursors. The calculated structures show that nitrate groups are stable in the lattice, and combined with the formation energies can be viewed a preferentially adopting the anion state.

Conclusive assignment of the presence of these acceptors may be found from the characteristic vibrational modes that these complexes give rise to.

References

[1] S. Limpijumnong, S. B. Zhang, S.-H.. Wei, and C. H. Park, Phys. Rev. Lett. **92**, 155504 (2004).
[2] D. M. Bagnall, Y. F. Chen, , Z. Zhu, T. Yao, S. Koyama, M. Y. Shen, and T. Goto, Appl. Phys. Lett. **70**, 2230 (1997).
[3] Z. K. Tang, G. K. L. Wong, M. Yu, P. Kawasaki, A. Ohtomo, H. Koinuma, and Y. Segawa, Appl. Phys. Lett. **72**, 464 (1998).
[4] D. K. Hwang, S. H. Kang, J. H. Lim, E. J. Yang, J. Y. Oh, J. H. Yang, and S. J. Park, Appl. Phys. Lett. **86**, 222101 (2005).
[5] A. Kobayashi, O. F. Sankey, and J. D. Dow, Phys. Rev. B **28**, 946 (1983).
[6] C. H. Park, S. B. Zhang, and S.-H. Wei, Phys. Rev. B **66**, 073202 (2002).
[7] D. C. Look, D. C. Reynolds, C. W. Litton, R. L. Jones, D. B. Eason, and G. Cantwell, Appl. Phys. Lett. **80**, 1830 (2002).
[8] J. M. Bian, X. M. Li, C. Y. Zhang, W. D. Yu, and X. D. Gao, Appl. Phys. Lett. **85**, 4070 (2004).
[9] I. V. Rogozin, Thin. Solid. Films. **4**, 4318 (2008).
[10] W. Wei, L. Kerr, and N. Leyarovska, Chem. Phys. Lett. **469**, 318 (2009).
[11] S. B. Zhang, S.-H. Wei, and A. Zunger, Phys. Rev. B **63**, 075205 (2001).
[12] A. Tsukazaki, A. Ohtomo, T. Onuma, M. Ohtani, T. Makino, M. Sumiya, S. F. Ohtani, K. Chichibu, S. Fuke, Y. Segawa, H. Ohno, H. Koinuma, and M. Kawasaki, Nature Mater. **4**, 42 (2005).
[13] K.-K. Kim, H.-S. Kim, D.-K. Hwang, J.-H. Lim, and S.-J. Park, Appl. Phys. Lett. **83**, 63 (2003).
[14] Y. R. Ryu, S. Zhu, D. C. Look, J. M. Wroble, H. M. Jeong, H. W. White, J. Cryst. Growth **216**, 330 (2000).
[15] A. Allenic, W. Guo, Y. B. Chen, G. Y. Zhao, X. Q. Pana, Y. Che, Z. D. Hu, B. Liu, J. Mater. Res. **22**, 2339 (2007)
[16] Y. R. Ryua, T. S. Lee, J. H. Leem, and H. W. White, Appl. Phys. Lett. **83**, 4032 (2003).
[17] H. W. Liang, Y. M. Lu, D. Z. Shen, Y. C. Liu, J. F. Yan, C. X. Shan, B. H. Li, Z. Z. Zhang, J. Y. Zhang, X. W. Fan, Phys. Status Solidi A **202**, 1060 (2005).
[18] M. Pan, J. Nause, V. Rengarajan, R. Rondon, E. H. Park, I. T. Ferguson, J. Electron Mater **36**, 457 (2oo7).
[19] W. Liu, S. L. Gu, J. D. Ye, S. M. Zhu, Y. X. Wu, Z. P. Shan, R. Zhang, Y. D. Zheng, S. F. Choy, G. Q. Lo, X. W. Sun J. Cryst. Growth **310**, 2448 (2008).
[20] A. Zeuner, H. Alves, D. M. Hofmann, B. K. Meyer, A. Hoffmann, U. Haboeck, M. Strassburg, M. Dworzak, Phys. Status Solidi B **234**, r7 (2002).
[21] J. A. Aparicio, F. E. Fernandez, J. Mol. Struct. **10**, 46840 (2010).
[22] T. Monteiro, A. J. Neves, M. C. Carmo, M. J. Soares, M. peres, J. Wang, J. App. Phys. **98**, 013502 (2005).
[23] B. K. Meyer, H. Alves, D. M. Hofmann, W. Kriegseis, D. Forster, F. Bertram, J. Christen, A. Hoffmann, M. Strašsburg, M. Dworzak, U. Haboeck, A. V. Rodina, Phys. Solid State B **241**, 231 (2004).
[24] B. T. Adekore, J. M. Pierce, R. F. Davis, D. W. Barlage, J. F. Muth, J. Appl. Phys. **102**, 024908 (2007).
[25] N. Haneche, A. Lusson, C. Sartel, A. Marzouki, V. Sallet, M. Oueslati, F. Jomard, P. Galtier, Phys. Status Solidi **247**, 1671 (2009).
[26] J. L. Lyons, A. Janotti, and C. G. Van de Walle, Appl. Phys. Lett. **95**, 252105 (2009).
[27] E. -C. lee, Y. -S. Kim, Y. -G. Jin, K. J. Chang, Phys. Rev. B **64**, 085120 (2001).
[28] P. R. Briddon and R. Jones, Phys. Status Solidi B **217**, 131 (2000).
[29] M. J. Rayson and P. R. Briddon, Computer Phys. Comm. **178**, 128 (2008).
[30] H. J. Monkhorst and J. D. Pack, Phys. Rev. B **13**, 5188 (1976).
[31] N. Troullier and J. L. Martins, Phys. Rev. B **43**, 1993 (1991).
[32] J. P. Perdew and Y. Wang, Phys. Rev. B **45**, 13244 (1992).
[33] J. P. Goss, M. J. Shaw, and P. R. Briddon, Topics in Appl. Phys. **104**, 69 (2007).
[34] *CRC handbook of chemistry and physics*, 73 ed., edited by D. R. Lide (CRC, Boca Raton, FL, 1992).
[35] S. Lany, A. Zunger, Phys. Rev. B **64**, 235104 (2008).
[36] X. Li, Y. Yan, T. A. Gessert, C. DeHart, C. L. Perhins, D. Young, T. J. Coutts, Solid State Commun. **6**, 56 (2003).
[37] Y. Yan, S. B. Zhang, S. T. Pantelides, Phys. Rev. L. **86**, 5723 (2001).
[38] J. F. Rommeluere, L. Svob, F. Jomard, J. Mimila-Arroyo, G. Amiri, V. Lusson, V. Sallet, O. Gorochov, P. Galtier, Y. Marfaing, Phys. Status Solidi **1** 904 (2004).
[39] H. Oberhammer, J. Mol. Struct. **605**, 1439 (2002).
[40] N. H. Nickel, F. Friedrich, J. F. Rommelure, P. Galtier, Appl. Phys. Lett. **87**, 211905 (2005).
[41] L. L. Kerr, X. Li, M. Canepa, A. J. Sommer, Thin Solid Films **515**, 5282 (2007).
[42] W. A. Brown, D. A. King, J. Phys. Chem. B **104**, 2578 (2000).